

CYCLIC SPATIAL FILTERING IN RADIO ASTRONOMY: APPLICATION TO LOFAR DATA

Rym Feliachi¹, Rodolphe Weber¹, Albert-Jan Boonstra²

¹Institut PRISME, University of Orléans
Site Galilée, 12 rue de Blois, 45067 Orléans cedex 2, France
email: rym.feliachi@univ-orleans.fr, rodolphe.weber@univ-orleans.fr

²ASTRON, P.O. Box 2, 7990 AA Dwingeloo, Netherlands
email: boonstra@astron.nl

ABSTRACT

Radio astronomical observations are increasingly corrupted by radio frequency interference, and real-time filtering algorithms are becoming essential. New generations of radio telescopes will be based on antenna arrays providing the possibility of applying spatial filtering techniques. In this paper we compare the performance of two different approaches based on subspace decomposition of respectively the classical array correlation matrix and the cyclic array correlation matrix. This comparison is done through simulation on synthetic data and through simulations on real data acquired with the new generation low frequency array radio telescope LOFAR.

I. INTRODUCTION

For several years, radio astronomy has had to face two contradictory trends. On the one hand, the exponential expansion of telecommunications has generated a growing demand on the electromagnetic spectrum, reducing the bandwidths available for good quality radio astronomical observations. On the other hand, radio astronomical needs in terms of sensitivity and bandwidth have also grown. As a result, radio frequency interference (RFI) mitigation has become a significant issue for current and future radio telescopes.

The various methods that have been tried to limit RFI depend on the type of interference and the type of instruments. Time, frequency and/or spatial properties can be considered in order to find efficient excision processing techniques [1]. A desirable property of the RFI mitigation algorithms is that they are, to a certain extent, generic so that they can be applied to transmitters having different modulation schemes. Because of limited available resources, there are also limits to the complexity of the algorithm.

The design of the new generation of radio telescopes will be based on antenna arrays spanned



Figure 1: antennas of a low frequency radio telescope (LOFAR) station. The signals are combined by phased array beamforming and correlated with other LOFAR station signals. Sky images are produced by inverse Fourier transforming the correlation products.

over hundreds of kilometres. This is the case for the LOFAR telescope (see [2], figure 1 and section IV) which is a phased array radio interferometer, but it will also be the case for the SKA telescope [3] which will be a mix of phased antenna arrays and dish arrays.

In [4] and [5], it has been shown that the use of spatial filtering techniques can limit the impact of the incoming RFI for such radio telescopes. This method is based on the estimation of the RFI spatial signature vector from the correlation matrix followed by a subspace projection to remove that dimension from the correlation matrix. To preserve the integrity of the cosmic information, a correction matrix must be applied on the “cleaned” correlation matrix [6]. However, this method requires good calibration of the system, and in some cases has limited performance due to the presence of relatively strong cosmic sources. Besides, it is not well-suited for removing weak interferences.

In this framework, this paper evaluates a new method for the estimation of the RFI spatial signature vector. The proposed approach is based on RFI specific properties named cyclostationarity. Indeed, most of telecommunications signals present

a hidden periodicity which is usually scrambled by the intrinsic signal randomness [7]. For example, this hidden periodic characteristic can be generated by the carrier frequency or the baud rate of the incoming RFI. For array signal processing, cyclostationarity was introduced by Gardner [8]. In this analysis, the correlation matrices are replaced by the cyclic correlation matrices. The desired direction vector is derived from the eigenvector corresponding to the largest eigenvector of the cyclic correlation matrix. This has led to an improvement in existing MUSIC [9] and ESPRIT algorithms [10].

In this paper, we investigate the improvement of spatial filtering defined in [4, 5, 6] by using cyclic correlation matrices to find the RFI signature vectors. Section II describes the data model and the cyclic spatial filtering approach. The performance of the “classic” spatial filtering and the performance of the proposed cyclic filtering are compared in section III. Section IV presents the experimental setup and the results.

II. CYCLIC SPATIAL FILTERING

1. The data model

Consider a telescope array consisting of M antennas, each having a received signal $z_k(t)$, $k=1\dots M$. It is assumed that the narrowband condition holds and that geometric delays for each antenna and each impinging source can be represented by phase shifts. In this case, the telescope output vector $z(t)$ can be modeled in complex baseband form as:

$$z(t) = A_{sK_1} s(t) + A_{rK_2} r(t) + n(t) \quad (1)$$

where:

- $z(t) = [z_1(t), z_2(t), \dots, z_M(t)]^T$ is the $M \times 1$ vector of telescope signals at time t .
- $s(t) = [s_1(t), s_2(t), \dots, s_{K_1}(t)]^T$ is the $K_1 \times 1$ vector of K_1 white, Gaussian, independent cosmic source signals. $A_{sK_1} = [a_{s1}, a_{s2}, \dots, a_{sK_1}]$ is a $M \times K_1$ matrix where each a_{sk} , $k=1\dots K_1$, is the spatial signature of the corresponding cosmic source $s_k(t)$, $k=1\dots K_1$.
- $r(t) = [r_1(t), r_2(t), \dots, r_{K_2}(t)]^T$ is the $K_2 \times 1$ vector of K_2 cyclostationary RFI signals. $A_{rK_2} = [a_{r1}, a_{r2}, \dots, a_{rK_2}]$ is a $M \times K_2$ matrix where each a_{rk} , $k=1\dots K_2$, is the spatial signature of the corresponding RFI signal $r_k(t)$, $k=1\dots K_2$. It is assumed that these K_2 RFI signals have the same cyclostationary property. If not, the algorithm will be applied on each group of RFI

signals having the same cyclostationary property.

- $n(t)$ is the $M \times 1$ system noise vector with independent Gaussian entries. There is no specific assumption made concerning the whitening of the covariance matrix and calibration of the data. Also, no assumption is made on these noise powers relative to the cosmic source powers.

In order to remove RFI from the received data, we can filter them out by applying a spatial null in the direction of the undesired signals. Each received signal is identified by its spatial signature in the received data model. We can consequently project out these spatial signatures, if we can estimate them, as is explained in the following section.

2. Classical approach

When spatial signatures of RFI sources are unavailable, we can estimate them using an eigenvalue decomposition (EVD) of the estimated correlation matrix:

$$\hat{\mathbf{R}} = \left\langle z(t) z^H(t) \right\rangle_L = \mathbf{U} \mathbf{\Lambda} \mathbf{U}^H \quad (2)$$

where $\langle \cdot \rangle_L$ is a time averaging over L samples, \mathbf{U} is the eigenvector matrix, $\mathbf{\Lambda}$ is the eigenvalue matrix, and \cdot^H denotes complex conjugate transpose.

In this approach, the signal subspace (i.e. subspace formed by the eigenvectors associated to the largest eigenvalues) will span the same dimensions as the RFI signals, but only if the cosmic sources are negligible and the system noise is calibrated (whitened). The interference can be (spatially) suppressed by multiplying the observed correlation matrix $\hat{\mathbf{R}}$ with a projection matrix $\mathbf{P}^{\text{classic}}$ derived from the signal subspace of $\hat{\mathbf{R}}$ (cf. [4]).

3. Cyclic approach

According to [8], we can also estimate the spatial signatures using singular value decomposition (SVD) of the estimated cyclic correlation matrix $\hat{\mathbf{R}}^\alpha$:

$$\begin{aligned} \hat{\mathbf{R}}^\alpha &= \left\langle z(t) z^H(t) \exp(-j2\pi\alpha t) \right\rangle_L \\ &= \mathbf{U}_{\text{cyclic}} \mathbf{\Lambda}_{\text{cyclic}} \mathbf{V}_{\text{cyclic}}^H \end{aligned} \quad (3)$$

Here α is the cyclostationary parameter which characterizes the RFI signals, and is called the cyclic frequency. In some cases, the complex conjugate transpose can be replaced by a simple transpose operator.

Since the cosmic source signals $s(t)$ and the system noise signals $n(t)$ are not cyclostationary with cyclic frequency α , the cyclic correlation matrix will depend asymptotically on RFI only:

$$\hat{\mathbf{R}}^\alpha = \hat{\mathbf{R}}_{rK_2}^\alpha + \hat{\mathbf{R}}_{sK_1}^\alpha + \hat{\mathbf{R}}_n^\alpha \quad (4)$$

Consequently, the signal subspace formed by the K_2 largest singular vectors $\mathbf{U}_{rK_2} = [\mathbf{u}_1 \dots \mathbf{u}_{K_2}]$ will span the same subspace as the RFI spatial signatures \mathbf{A}_{rK_2} . Thus, unlike classical spatial filtering, where the interferer signal subspace may be affected by the cosmic sources and the system noise signals, here \mathbf{U}_{rK_2} spans the subspace formed only by the interferer spatial signatures \mathbf{A}_{rK_2} .

Once these spatial signatures have been estimated, we can filter out the RFI signals by applying a projector on the telescope output:

$$\mathbf{z}(t)_{\text{cleaned}} = \mathbf{P}_{\text{cyclic}} \mathbf{z}(t) \quad (5)$$

where $\mathbf{P}_{\text{cyclic}}$ is the cyclic spatial projector defined by: $\mathbf{P}_{\text{cyclic}} = \mathbf{I} - \mathbf{U}_{rK_2} \mathbf{U}_{rK_2}^H$, and \mathbf{I} is the $M \times M$ identity matrix.

Since \mathbf{A}_{rK_2} spans the same subspace as \mathbf{U}_{rK_2} , \mathbf{A}_{rK_2} can be written as a linear combination of $\mathbf{U}_{rK_2} \Rightarrow \mathbf{A}_{rK_2} = \mathbf{U}_{rK_2} \boldsymbol{\gamma}$ ($\boldsymbol{\gamma}$ is an arbitrary normalized vector). This leads to the following result when applying the projector on \mathbf{A}_{rK_2} :

$$\mathbf{P}_{\text{cyclic}} \mathbf{A}_{rK_2} = (\mathbf{I} - \mathbf{U}_{rK_2} \mathbf{U}_{rK_2}^H) \mathbf{U}_{rK_2} \boldsymbol{\gamma} = \mathbf{0} \quad (6)$$

Besides, the subspace spanned by \mathbf{A}_{sK_1} is orthogonal to one spanned by \mathbf{U}_{rK_2} , leading to:

$$\mathbf{P}_{\text{cyclic}} \mathbf{A}_{sK_1} = \mathbf{A}_{sK_1} \quad (7)$$

It follows that (5) becomes, using (6) and (7):

$$\begin{aligned} \mathbf{z}_{\text{cleaned}}(t) &= \mathbf{P}_{\text{cyclic}} (\mathbf{A}_{sK_1} \mathbf{s}(t) + \mathbf{n}(t)) \\ &= \mathbf{A}_{sK_1} \mathbf{s}(t) + \mathbf{P}_{\text{cyclic}} \mathbf{n}(t) \end{aligned} \quad (8)$$

This results in a *cleaned* output signals matrix. The bias induced by $\mathbf{P}_{\text{cyclic}}$ in Eq. 8 can be removed as explained in [6]. The next section will demonstrate by simulation the effectiveness of this approach through a comparison with the classical approach. Even though in practice there is no asymptotic situation, the simulations will clearly show the advantage of the cyclic approach.

III. PERFORMANCE

We consider the case where we have $K_1 = 1$ interferer and $K_2 = 1$ cosmic source, using a $M = 8$ antennas uniform linear configuration. The RFI is a BPSK signal with the following characteristics: the carrier frequency is $f_0 = 0.3$, the baud rate is $1/T_{\text{symbol}} = 1/8$, the emission filter is

rectangular, its power is σ_{r1}^2 and its spatial signature is \mathbf{a}_{r1} . The cosmic source power is σ_{s1}^2 . We assume identical noise powers for each telescope. Without loss of generality, the system noise power in the simulations for each antenna has been set to $\sigma_n^2 = 1$ (i.e. $E(\mathbf{n}(t) \mathbf{n}^H(t)) = \mathbf{I}$). We consider the correlation matrix defined by:

$$\mathbf{R} = \underbrace{\sigma_{r1}^2 \mathbf{a}_{r1} \mathbf{a}_{r1}^H}_{\mathbf{R}_{r1}} + \underbrace{\sigma_{s1}^2 \mathbf{a}_{s1} \mathbf{a}_{s1}^H + \sigma_n^2 \mathbf{I}}_{\mathbf{D}} \quad (9)$$

We define the Interference to Noise Ratio before any spatial filtering by:

$$INR_{\text{before}} = \frac{\text{tr}(\mathbf{R}_{r1})}{\text{tr}(\mathbf{D})} = \frac{\sigma_{r1}^2}{(\sigma_{s1}^2 + \sigma_n^2)} \quad (10)$$

We also define the Interference to Noise Ratio after spatial filtering by:

$$\begin{aligned} INR_{\text{after}} &= \frac{\text{tr}(\hat{\mathbf{P}}(\mathbf{R}_{r1})\hat{\mathbf{P}})}{\text{tr}(\mathbf{D})} \\ &= \frac{\sigma_{r1}^2 \text{tr}(\hat{\mathbf{P}} \mathbf{a}_{r1} \mathbf{a}_{r1}^H \hat{\mathbf{P}})}{M(\sigma_{s1}^2 + \sigma_n^2)} \end{aligned} \quad (11)$$

where $\hat{\mathbf{P}}$ is the estimated projector obtained through either the classical approach ($\mathbf{P}_{\text{classic}}$) or the cyclic approach ($\mathbf{P}_{\text{cyclic}}$).

Figure 2 shows the computed INR_{after} as a function of the INR_{before} . The projector $\hat{\mathbf{P}}$ is estimated from time series with length $L = 8192$. We have also used different ratios between the cosmic source power and the system noise power in the total noise

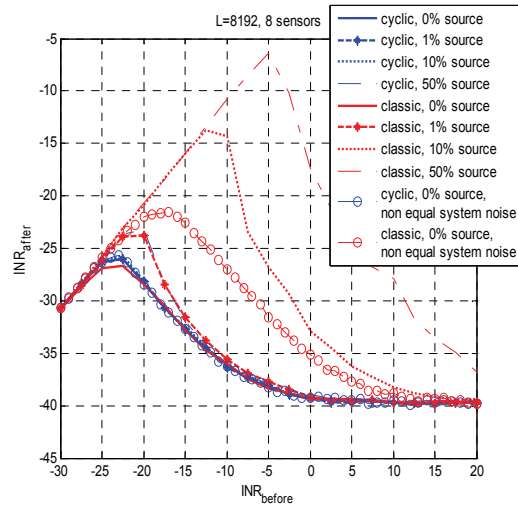


Figure 2 - Simulation results of the INR before and after applying spatial filtering, for 8192 samples and 8 antennas. The first 8 curves satisfy the “noise equal powers” assumption. For the last 2 curves, the noise powers fluctuate within 20% between antennas.

power contribution. For example, a 50% contribution indicates that the system noise and the cosmic source have the same power.

When the projector is badly estimated, the RFI is not filtered out, then, apart from a small bias, $INR_{after} = INR_{before}$. This bias (≈ 0.6 dB) can be explained by the fact that even though the interferer spatial signature is wrongly estimated, the projector will remove a subspace dimension and hence some energy. When the number of antennas increases, this offset decreases.

When we have only system noise (i.e. 0% source), the two methods yield similar simulation results. Indeed, in the classic (asymptotic) approach, the estimated eigenvector does not depend on the (whitened) noise power, assuming equal noise powers for each of the antennas.

However as we add a cosmic source, differences between the two approaches become apparent. This result can be explained by the fact that in the classic spatial filtering case, unlike the cyclic case, the estimated largest eigenvector is influenced by the source. Similar results are observed when the previous “equal noise powers” assumption is not satisfied (see the last 2 curves on figure 2).

For large INR_{before} we retrieve an extreme case [9]:

$$INR_{after} = \frac{1}{L} \left(1 + \frac{1}{M INR_{before}} \right) \quad (12)$$

For $L = 8192$, the theoretical limit (Eq. 12) is -39.09 dB, which is closely approached in the simulation: -39.83 dB.

In figure 3, performance and limitations of both classic and cyclic spatial filtering for the 50% source case are shown. We compute the inner product between the true RFI spatial signature \mathbf{a}_1 and the estimated one (the strongest eigenvector \mathbf{u}_1) according to the variations of the INR (as defined in Eq. 10).

For $INR > 0$ dB, \mathbf{u}_1 is very close to the true spatial signature of the interferer in both cases. Indeed, the total noise power contribution (the cosmic source + system noise) is (much) less than the power of the RFI. Thus, the first eigenvalue is dominated by the RFI, and the corresponding eigenvector relates to a direction vector pointing in the direction of the RFI.

As the INR decreases, the performance of the classic approach drops off. Indeed, \mathbf{u}_1 is gradually altered by the cosmic source contribution. Thus, below an INR of -5 dB, the spatial signature of the interferer is poorly estimated. This decreasing

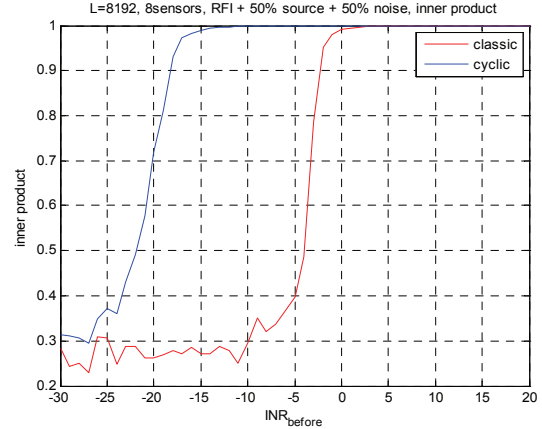


Figure 3 - Simulation results of the inner product between the true RFI spatial signature and the estimated one, for 8192 samples and 8 antennas. This inner product is equal to 1 if the spatial signature is accurate.

performance is consistent with the results shown in figure 2.

The cyclic approach is more robust to this cosmic source contribution. Indeed, the RFI spatial signature is still well estimated at $INR = -15$ dB.

The simulations above show that, for low INR, and in the presence of a cosmic source, the cyclic method outperforms the classic one. In the next section, we will demonstrate experimentally that the cyclic method also has advantages over the classic spatial filtering approach for large INR.

IV. EXPERIMENTAL RESULTS

We have applied the classic and cyclic spatial filtering to real observations acquired with the LOFAR radio telescope. LOFAR is a phased array interferometric telescope developed by ASTRON in the Netherlands. It is currently in the roll-out phase and operates in the band 30-240 MHz [2]. In LOFAR, antennas are grouped in so-called stations in which the signals of ~ 100 antennas are combined using phased-array beamforming. The beamformed signals of many stations are combined centrally by correlating them. Sky images are produced by inverse Fourier transforming the correlation products.

We have observed in the 160-240 MHz LOFAR band, which contains a very strong transmitter (pager) at 170 MHz with an INR of 47 dB. The array configuration consisted of $M=8$ LOFAR antennas. Figure 4 shows the eigenvalues obtained from the classic and the cyclic correlation matrix (resp. $\hat{\mathbf{R}}$ and $\hat{\mathbf{R}}^\alpha$) which were derived from baseband data of the antennas of one station. The cyclic frequency, α , of the pager has been first

estimated from the data: $\alpha=0.1221$ in normalized frequency.

The figure shows that the interferer signal subspace can be fairly well estimated using one dimension in the cyclic decomposition, whereas it needs two dimensions in the classic one. The more dimensions are used to remove the interferer, the more information about the cosmic sources is thrown away as well. We used therefore only the eigenvector corresponding to the strongest eigenvalue to build the projector for both methods.

Figure 5 shows the effect of the projector on the pager. Using the cyclic method, the pager is removed more effectively compared with the classic approach. The main reason is that the spatial filter is applied to uncalibrated data; unlike the classic spatial filter, the cyclic method is not dependent on calibration. The achieved attenuation of 35 dB is quite large, but does not reach the theoretical limit. The reason for this probably is a multipath effect which influences the interferer subspace of the covariance matrix; alternatively, there may also be a second, weaker, transmitter present at a larger distance.

V. CONCLUSION

In this paper, we have described cyclic spatial filtering. This method seems to be an attractive alternative to the classic method. Indeed, as shown with simulations and experimental results, it leads to better performance for cases where there are relatively strong cosmic sources or for cases where the arrays are uncalibrated.

VI. REFERENCES

[1] P. A. Fridman & W. A. Baan, "RFI mitigation methods in radio astronomy", *Astronomy and Astrophysics*, 378, 327-344, October 2001
 [2] Low Frequency array for radio astronomy <http://www.lofar.org/>
 [3] Square Kilometer Array <http://www.skatelescope.org/>
 [4] A. Leshem, A.-J. van der Veen, and A.-J. Boonstra, "Multichannel interference mitigation techniques in radio astronomy," *Astrophys. J. Supplement Series*, vol. 131, pp. 355–373, Nov. 2000.
 [5] J. Raza, A.J. Boonstra, and A.J. van der Veen, "Spatial filtering of RF interference in radio astronomy," *IEEE Signal Processing Letters*, vol. 9, no 2, pp. 64-67, February 2002.
 [6] S. van der Tol and A. van der Veen, "Performance analysis of spatial filtering of RF interference in radio astronomy" *IEEE Transactions on Signal Processing*, vol. 53, 2005, pp. 896-910.

[7] E. Serpedin, F. Panduru, I. Sari, and G.B. Giannakis, "Bibliography on cyclostationarity," *Signal Processing*, vol. 85, Dec. 2005, pp. 2233-2303.
 [8] W.A. Gardner, "Simplification of MUSIC and ESPRIT by exploitation of cyclostationarity", *Proc. of IEEE* vol.76, n° 7, p. 845-847, 1988
 [9] R. O. Schmidt, « Multiple Emitter Location and Signal Parameter Estimation », *IEEE ASSP*, vol. 4, n° 3, p. 273-280, 1983.
 [10] R. Roy, and T.Kailath, "ESPRIT—Estimation of signal parameters via rotational invariance techniques," *IEEE Trans. Acoust., Speech, Signal Processing*, Vol. 37, No. 7. (1989), pp. 984-995.

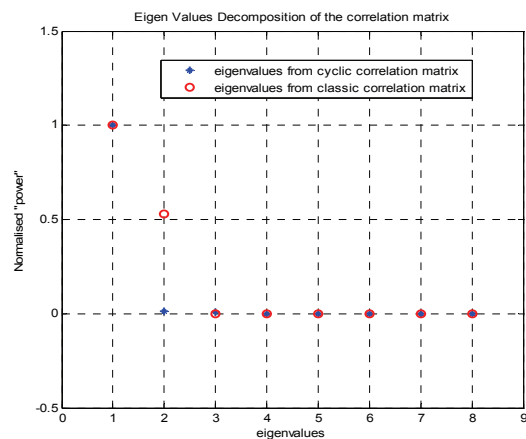


Figure 4 – The eigenvalue decomposition of the classic and the cyclic correlation matrix estimated from real data acquired with the LOFAR telescope. A strong transmitter is present in the dataset (see figure5). $M=8$ antennas have been used and the correlation matrices have been estimated over $L=65536$ samples.

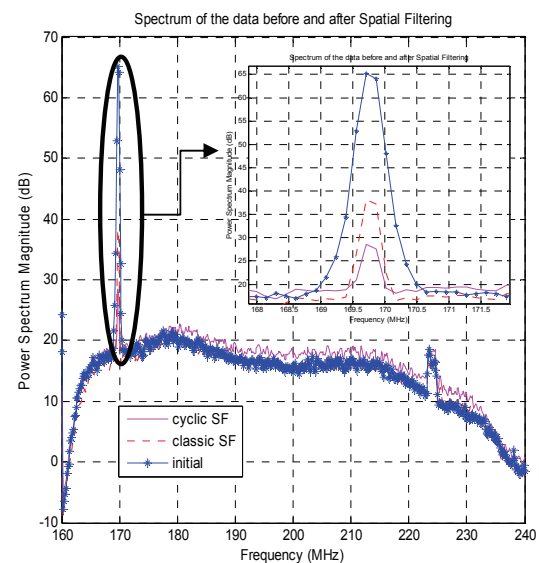


Figure 5 – Spectrum of one antenna output after applying cyclic and classic spatial filtering ($M=8$, $L=65536$).